MOLECULAR AND CELLULAR BIOLOGY, June 2004, p. 5080–5087 Vol. 24, No. 11
0270-7306/04/$08.00+0 DOI: 10.1128/MCB.24.11.5080–5087.2004

Increased Insulin Sensitivity and Reduced Adiposity in Phosphatidylinositol 5-Phosphate 4-Kinase $\beta^{-/-}$ Mice

Katja A. Lamia,[1] Odile D. Peroni,[2] Young-Bum Kim,[2] Lucia E. Rameh,[3] Barbara B. Kahn,[2] and Lewis C. Cantley[1]*

Division of Signal Transduction, Beth Israel Deaconess Medical Center, and Department of Cell Biology, Harvard Medical School,[1] and Division of Endocrinology, Diabetes, and Metabolism, Beth Israel Deaconess Medical Center, and Department of Medicine, Harvard Medical School,[2] Boston, and Boston Biomedical Research Institute, Watertown,[3] Massachusetts

Received 25 November 2003/Returned for modification 5 January 2004/Accepted 16 March 2004

Phosphorylated derivatives of the lipid phosphatidylinositol are known to play critical roles in insulin response. Phosphatidylinositol 5-phosphate 4-kinases convert phosphatidylinositol 5-phosphate to phosphatidylinositol 4,5-*bis*-phosphate. To understand the physiological role of these kinases, we generated mice that do not express phosphatidylinositol 5-phosphate 4-kinase β. These mice are hypersensitive to insulin and have reduced body weights compared to wild-type littermates. While adult male mice lacking phosphatidylinositol 5-phosphate 4-kinase β have significantly less body fat than wild-type littermates, female mice lacking phosphatidylinositol 5-phosphate 4-kinase β have increased insulin sensitivity in the presence of normal adiposity. Furthermore, in vivo insulin-induced activation of the protein kinase Akt is enhanced in skeletal muscle and liver from mice lacking phosphatidylinositol 5-phosphate 4-kinase β. These results indicate that phosphatidylinositol 5-phosphate 4-kinase β plays a role in determining insulin sensitivity and adiposity in vivo and suggest that inhibitors of this enzyme may be useful in the treatment of type 2 diabetes.

Type 2 diabetes affects a large and growing population in the developed world. This disease is characterized by resistance to many metabolic actions of insulin. Failure of pancreatic beta cells to compensate leads to hyperglycemia and disordered lipid metabolism. Obesity is a major risk factor for type 2 diabetes, and the majority of people with type 2 diabetes are obese. Although new therapeutic agents have greatly improved the management of type 2 diabetes, currently available treatments remain inadequate.

Although many molecules have been implicated in insulin signaling in ex vivo or in in vitro systems, relatively few have been shown to affect glucose homeostasis in vivo (22). Not surprisingly, genetic disruption of the insulin receptor or insulin receptor substrates (e.g., IRS-1) has been shown to reduce whole-body insulin responsiveness (2, 3, 30). In addition, mice lacking protein tyrosine phosphatase 1B, which dephosphorylates the insulin receptor and insulin receptor substrates (15), are lean and have enhanced insulin sensitivity in vivo (13, 20). Also, genetic manipulation of the phosphoinositide 3-kinase (PI3K) signaling pathway in mice has been shown to affect insulin sensitivity. Mice with reduced levels of p85 regulatory subunits of PI3K (which can exert a negative effect on the pathway) have increased insulin sensitivity (14, 23, 31, 33). Deletion of Akt2, a protein serine/threonine kinase that is activated by the PI3K-generated second messenger phosphatidylinositol 3,4,5-*tris*-phosphate (PI-3,4,5-P_3), results in impaired insulin signaling in mice (10). Finally, disruption of the gene encoding SHIP2, a phosphatase that degrades PI-3,4,5-P_3, results in a dramatic increase in insulin sensitivity in mice (11).

Aberrant regulation of other phosphoinositides, such as phosphatidylinositol 4,5-*bis*-phosphate (PI-4,5-P_2), may contribute to diabetes and obesity. For example, PI-4,5-P_2 is the substrate used by PI3K for synthesis of PI-3,4,5-P_3. In addition, PI-4,5-P_2 regulates the function of the Tubby protein. Mice with mutations in the *tubby* gene develop maturity-onset obesity and diabetes (6, 28).

The bulk of PI-4,5-P_2 in mammalian cells is synthesized from phosphatidylinositol 4-phosphate (PI-4-P) (35). A few years ago, it was shown that the type II phosphatidylinositol phosphate kinases produce PI-4,5-P_2 by an alternative route, namely, via phosphatidylinositol 5-phosphate (PI-5-P) (26), and they are now called phosphatidylinositol 5-phosphate 4-kinases (PI-5-P4-kinases). PI-5-P is far less abundant than PI-4-P or PI-4,5-P_2, and relatively little is known about its function or regulation. Some recent results indicate a role for PI-5-P in the regulation of PI3-kinase signaling: two groups demonstrated that the bacterial phosphatase IpgD, which was previously known to be required for Akt activation upon invasion, is a lipid phosphatase that produces PI-5-P from PI-4,5-P_2 (21, 25, 29, 32). Mammals have three isoforms of PI-5-P 4-kinase (PI5P4Kα, PI5P4Kβ, and PI5P4Kγ) encoded by distinct genes (9, 12, 17), and it was recently shown that overexpression of any of these three enzymes diminishes the insulin-stimulated activation of Akt by reducing the amount of PI-3,4,5-P_3 produced after insulin stimulation (8). These enzymes have different but overlapping tissue distributions. To assess the physiological importance of PI5P4Kβ, we generated mice lacking this protein. PI5P4K$\beta^{-/-}$ mice were found to have increased

* Corresponding author. Mailing address: Beth Israel Hospital, Harvard Institutes of Medicine, Division of Signal Transduction, 10th Floor, 330 Brookline, MA 02215. Phone: (617) 667-0947. Fax: (617) 667-0957. E-mail: lewis_cantley@hms.harvard.edu.

insulin sensitivity, reduced growth rates, and lower fat content than wild-type littermates. The observed insulin hypersensitivity is consistent with a role for the PI-5-P pathway in regulating PI 3-kinase signaling downstream of the insulin receptor.

MATERIALS AND METHODS

Generation of PI5P4Kβ$^{-/-}$ mice. Embryonic stem cells harboring a disruption in PI5P4Kβ were obtained from Lexicon Genetics, Inc. (clone 39557) (36). These cells were grown and expanded in our laboratory and were injected into blastocysts at the Beth Israel Deaconess Transgenic Facility. Three chimeric mice were obtained, and each was mated with two C57BL/6 female mice. Heterozygous mice derived from these crosses were mated to establish our colony in the C57BL/6 × 129Sv/Ev mixed genetic background.

PCR. For genotyping, a set of three primers was used to amplify regions of genomic DNA present in either wild-type samples or knockout samples. We used a single antisense primer (pR: ACC ATC CCA AAG CAC CCA GGA CC) corresponding to intron sequence downstream of the insertion site and two sense primers, one corresponding to intron sequence upstream of the insertion (pwtF: CGT GCT ATG CCG TCG TCG TTT CC) and the other within the 3′ end of the Lexicon insertion (pkoF: AGA AGC GAG AAG CGA ACT GAT TGG). The primer pair pwtF/pR amplifies a fragment of 598 bp, and the primer pair pkoF/pR amplifies a fragment of 496 bp. We used the recommended cycling conditions for Perkin Elmer AmpliTaq Gold with an annealing temperature of 56°C.

RT-PCR. cDNA derived from the endogenous PI5P4Kβ transcript was prepared by using a primer complementary to 29 bases in exon VIII of PI5P4Kβ (5′-CCT CGT CCT CTG CCC GCT CCT CCA CCT CC-3′). A fragment corresponding to bases 51 to 902 of the endogenous coding sequence was amplified using a forward primer from exon I (5′-CGC CAG CAA GAC AAG ACC AAG AAG AAG-3′) and a reverse primer to exon VIII (5′-CGC TCC TCC ACC TCC ATC TCC TCC-3′).

cDNA derived from the hybrid transcript produced by splicing the first exon of PI5P4Kβ to the 5′ cassette of the Lexicon retroviral insertion vector was prepared with a primer complementary to the βgeo sequence within the Lexicon vector. A fragment from the hybrid transcript was amplified with the forward primer from exon I (described above) and a nested reverse primer from the βgeo sequence in the Lexicon insertion vector (5′-GCA TCC TTC AGC CCC TTG TTG-3′).

Production of PI5P4Kβ antibody. PI5P4Kβ was cloned into the pGEX-4T-2 bacterial glutathione *S*-transferase fusion expression vector. GST-PI5P4Kβ was expressed in *Escherichia coli* strain DH5α, purified on glutathione-agarose beads, and cleaved with 2.5 U of thrombin (Sigma product no. T6634) per mg of fusion protein. Thrombin was removed from the solution by incubation with 20 μl of *p*-aminobenzamidine agarose beads (Sigma product no. A7155). Soluble, cleaved PI5P4Kβ was injected into rabbits at Pocono Rabbit Farm and Laboratory for antibody production. Anti-PI5P4Kβ antibodies were purified from 10 ml of rabbit serum on a column of untagged bacterially expressed PI5P4Kβ covalently attached to CNBr-activated Sepharose (Sigma product no. C9142).

Tissue lysate preparation and Western blotting. Tissue lysates were prepared by homogenizing tissues flash frozen in liquid nitrogen with a Tissue Tearor homogenizer in 400 to 750 μl of ice-cold buffer containing 50 mM HEPES (pH 7.4), 138 mM KCl, 4 mM NaCl, 1% NP-40, 50 mM sodium pyrophosphate, 100 mM sodium fluoride, 10 mM EDTA, 10 mM sodium orthovanadate, protease inhibitor pellets (Roche product no. 1873580), and 1 mM phenylmethylsulfonyl fluoride. After homogenization, the samples were incubated for 1 to 4 h at 4°C and then centrifuged for 10 min at 16,000 × *g*. Protein concentrations in lysates from adipose tissues were determined by subjecting an aliquot to precipitation by 10% trichloroacetic acid. Protein concentrations in other tissue lysates were determined by the Lowry method. For Western blotting, 40 to 100 μg of total protein was loaded per lane.

In vivo insulin stimulation. Either saline control or 0.5 U of Novolin-R per kilogram of body weight was administered to 5-month-old female mice by tail vein injection. The mice were sacrificed by cervical dislocation 5 min after the injection of saline or insulin and quickly dissected, and the tissues were flash frozen in liquid nitrogen.

Akt activity assays. Akt protein was immunoprecipitated from 500 μg of total lysate by incubation with 2 μg of an anti-Akt polyclonal antibody that recognizes both Akt1 and Akt2 (Upstate Biotechnology) coupled to protein G Sepharose for 4 h at 4°C. The immune pellets were washed three times in buffer containing 20 mM Tris (pH 7.5), 5 mM EDTA, 10 mM $Na_4P_2O_7$, 100 mM NaF, 2 mM Na_3VO_4 and 1% NP-40 and then twice in 50 mM Tris (pH 7.5), 10 mM $MgCl_2$, and 1 mM dithiothreitol. The beads were resuspended in 50 μl of kinase mixture (50 mM Tris [pH 7.5], 10 mM $MgCl_2$, 1 mM dithiothreitol, 5 μM ATP, 1 μM protein kinase inhibitor, 30 μM Crosstide (peptide substrate for Akt), and 2 μCi of [γ-^{32}P]ATP) and incubated for 30 min at 30°C. Samples (40 μl) were spotted onto phosphocellulose p81 paper and washed four times with 75 mM orthophosphoric acid and once with acetone. Radioactivity incorporation was determined by scintillation counting.

Weight measurements. Mice were weighed daily between the ages of 9 and 21 days, every 3 days between the ages of 21 and 54 days, and weekly between the ages of 8 and 26 weeks.

Insulin tolerance tests. Mice were placed in clean cages (without food) at 9:00 a.m. and were injected intraperitoneally at 1:00 p.m. on the same day with Novolin-R at a dosage of 0.5 to 0.75 U per kg of body weight. Blood glucose was measured with a One Touch Basic glucose meter before injection of insulin and at 15, 30, 45, 60, and 90 min following insulin injection.

Glucose tolerance tests. Mice were placed in clean cages (without food) at 7:00 p.m. on the day prior to the experiment. At 9:00 a.m. the following day, the mice were injected with 1 mg of glucose per g of body weight from a 20-mg/ml solution of glucose in 0.9% NaCl (autoclaved and filtered). Blood glucose levels were measured with a One Touch Basic glucose meter before the injection of glucose and at 10, 20, 30, 60, 120, and 180 min following glucose injection.

Body composition analysis. Mice were euthanized by CO_2 asphyxiation, and the stomach and intestines were removed with care to leave the attached fat behind. The wet carcasses were weighed and then dried for 3 to 10 days in a ventilated 60°C oven. The fully dried carcasses (determined by weight stabilization) were placed in a solution of 2 parts ethanol to 1 part 30% potassium hydroxide (KOH) and returned to the 60°C oven for 3 to 10 days, until the carcasses were fully saponified (determined by lack of fat droplets in solution). The carcass lysate volumes were normalized to 100 to 300 ml and analyzed for triglyceride content by using reagent A (Sigma product no. 337-40-A).

Measurement of food intake. Food intake was measured by housing one or two mice of the same genotype per cage and weighing the food in the cages every morning at 9:00 a.m. and every evening at 6:00 p.m. for 2 weeks. The difference between weighings was divided by the number of mice in the cage, and each cage was treated as a single sample for statistical analysis. The amount of food consumed was divided by the average body weight of the mice in each cage to determine the food intake normalized to total body weight.

Insulin and leptin measurements. Serum insulin and serum leptin levels were measured in duplicate or triplicate by using enzyme-linked immunosorbent assay reagents from Crystal Chem Inc. (catalog no. 90060 and 90030).

High-fat diet. Mice were placed on a high-fat diet beginning at the time of weaning (3 weeks of age). We used a synthetic diet prepared by Harlan Teklad (Madison, Wis.; catalog no. TD 93075), which contains 55% fat and 24% carbohydrate by calories.

Statistical analysis. Body weight growth curves, insulin and glucose tolerance tests, and food intake were analyzed by repeated-measures analysis of variance. Body composition, bone lengths, and bone mineral density were analyzed by Student's *t* test. All analyses were performed with StatView 4.1 software.

RESULTS

Generation of PI5P4Kβ$^{-/-}$ mice. We obtained from Lexicon Genetics, Inc., mouse embryonic stem cells in which retroviral insertion resulted in an integration event between exon I and exon II of the PI5P4Kβ gene. We determined that the Lexicon vector was inserted 818 bp downstream of the PI5P4Kβ ATG initiation codon and preserved the surrounding intron sequences without deletion (Fig. 1A). Primers surrounding the site of insertion were used to genotype mice by PCR (Fig. 1B). Mice derived from these cells that were homozygous for the PI5P4Kβ disruption (PI5P4Kβ$^{-/-}$ mice) were viable at slightly less than Mendelian ratios, allowing further characterization. (Of 987 pups born to heterozygous parents, 29% were wild type, 55% were PI5P4Kβ$^{+/-}$, and 16% were PI5P4Kβ$^{-/-}$.)

Since the Lexicon gene trap strategy is based on the disruption of splicing, we examined RNA from mouse brains to determine whether the full-length PI5P4Kβ RNA transcript

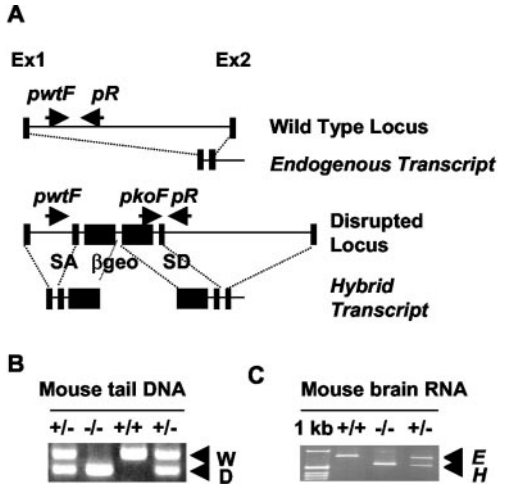

FIG. 1. Generation of PI5P4Kβ$^{-/-}$ mice. (A) Schematic representation of the PI5P4Kβ locus before and after insertion of the retroviral gene trap. Expression of the trapped gene is disrupted because the inserted sequence causes the endogenous transcript to be divided into two separate transcripts, neither of which can produce the endogenous protein. SA, splice acceptor sequence; βgeo, β-galactosidase and neomycin resistance cassette; SD, splice donor sequence. Primers used for genotyping by PCR are pkoF, pwtF, and pR. (B) PCR analysis of genomic DNA prepared from mouse tails. A 598-bp product (W) represents the wild-type allele; a 496-bp product (D) represents the disrupted allele. (C) RT-PCR analysis of RNA prepared from mouse brains. An 852-bp product (*E*) represents the endogenous transcript; a 613-bp product (*H*) represents the hybrid transcript formed by splicing of exon I to the gene trap sequence.

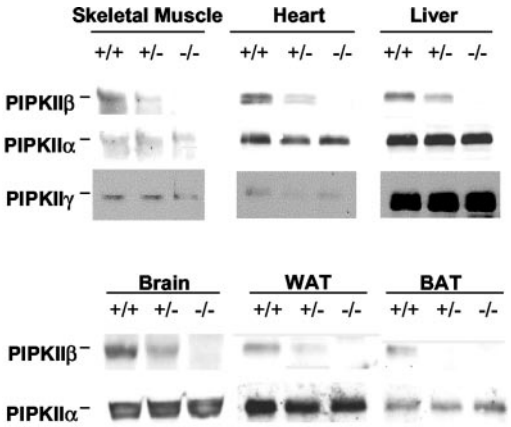

FIG. 2. Loss of PI5P4Kβ protein in tissues. Western blots for PI5P4Kβ, PI5P4Kα, and PI5P4Kγ protein levels in skeletal muscle, heart, liver, brain, white adipose tissue (WAT), and brown adipose tissue (BAT) are shown.

was suppressed in the PI5P4Kβ$^{-/-}$ mice. The endogenous transcript was undetectable in RNA prepared from the brains of homozygous mice, while it was easily detected in RNA prepared from the brains of both wild-type and heterozygous mice. We were able to detect the hybrid transcript expressed from the Lexicon gene trap vector in both heterozygous and homozygous mouse brain RNA (Fig. 1C).

We examined PI5P4Kβ protein levels using an anti-PI5P4Kβ antibody that we produced. We found PI5P4Kβ protein to be absent from all tissues examined from mice homozygous for the Lexicon disruption. We also examined the expression levels of PI5P4Kα and PI5P4Kγ and found that the expression of these genes was not upregulated to compensate for the loss of PI5P4Kβ (Fig. 2).

PI5P4Kβ$^{-/-}$ mice are hypersensitive to insulin. Since PI5P4Kβ is expressed in insulin-responsive tissues and phosphoinositide signaling plays a major role in insulin responses, we performed insulin and glucose tolerance tests on the PI5P4Kβ$^{-/-}$ mice. Both male and female mice with disruption of PI5P4Kβ were more sensitive to insulin than their wild-type littermates, and this trend increased as the mice aged (Fig. 3A). We also found that while the PI5P4Kβ null mice had normal glucose tolerance, they produced less insulin during the glucose tolerance test than did their wild-type littermates, confirming their increased insulin sensitivity (Fig. 3B). The histology of pancreatic islets is normal in mice lacking PI5P4Kβ, and they are normoglycemic under fasting and fed conditions (data not shown) as well as during the glucose tolerance test, indicating that pancreatic beta cell function is normal.

Insulin signaling is enhanced in skeletal muscles from PI5P4Kβ$^{-/-}$ mice. Multiple factors contribute to glucose clearance in response to insulin. To determine whether the increased insulin sensitivity observed in the absence of PI5P4Kβ could be attributed to increased signaling in response to insulin in individual tissues, we injected mice with a subsaturating dose of insulin and measured the activation of Akt in multiple insulin-responsive tissues. We found that insulin-stimulated Akt phosphorylation and activation are significantly increased by more than 50% in skeletal muscles and by ~25% in livers from mice lacking PI5P4Kβ compared to wild-type littermates. In contrast, Akt activation in response to insulin in white adipose tissue is not affected by the loss of PI5P4Kβ (Fig. 4).

PI5P4Kβ$^{-/-}$ mice are small and lean. We found that mice lacking PI5P4Kβ are 15 to 25% lighter than their wild-type littermates before weaning. After weaning, the weight difference between wild-type and PI5P4Kβ$^{-/-}$ female mice decreases and stabilizes around 10% in adults. However, the weight difference between wild-type and PI5P4Kβ$^{-/-}$ male mice continually increases and reaches 30% by 18 weeks of age (Fig. 5).

To further characterize the observed weight differences, we used a dual energy X-ray absorption scanner (DEXAScan). DEXAScan data allow the approximate calculation of total body fat content and bone mineral density and also provide a low-resolution X-ray picture of each mouse from which it is possible to measure the lengths of the long bones.

We found that the spines of male PI5P4Kβ$^{-/-}$ mice are 5.8% ± 0.3% shorter than those of wild-type littermates (P = 0.004 in the t test) and the femurs of male PI5P4Kβ$^{-/-}$ mice are 7.3% ± 0.7% shorter than those of wild-type littermates (P = 0.004) at 10 weeks of age. We also found that 10-week-old male PI5P4Kβ$^{-/-}$ mice have reduced bone mineral density (9.5% ± 0.7% lower than wild type; P = 0.001). This may be a consequence of their reduced body weight. Similar results were obtained for female mice at 10 weeks of age.

We also found that both male and female mice lacking PI5P4Kβ had normal amounts of fat at 10 weeks of age but

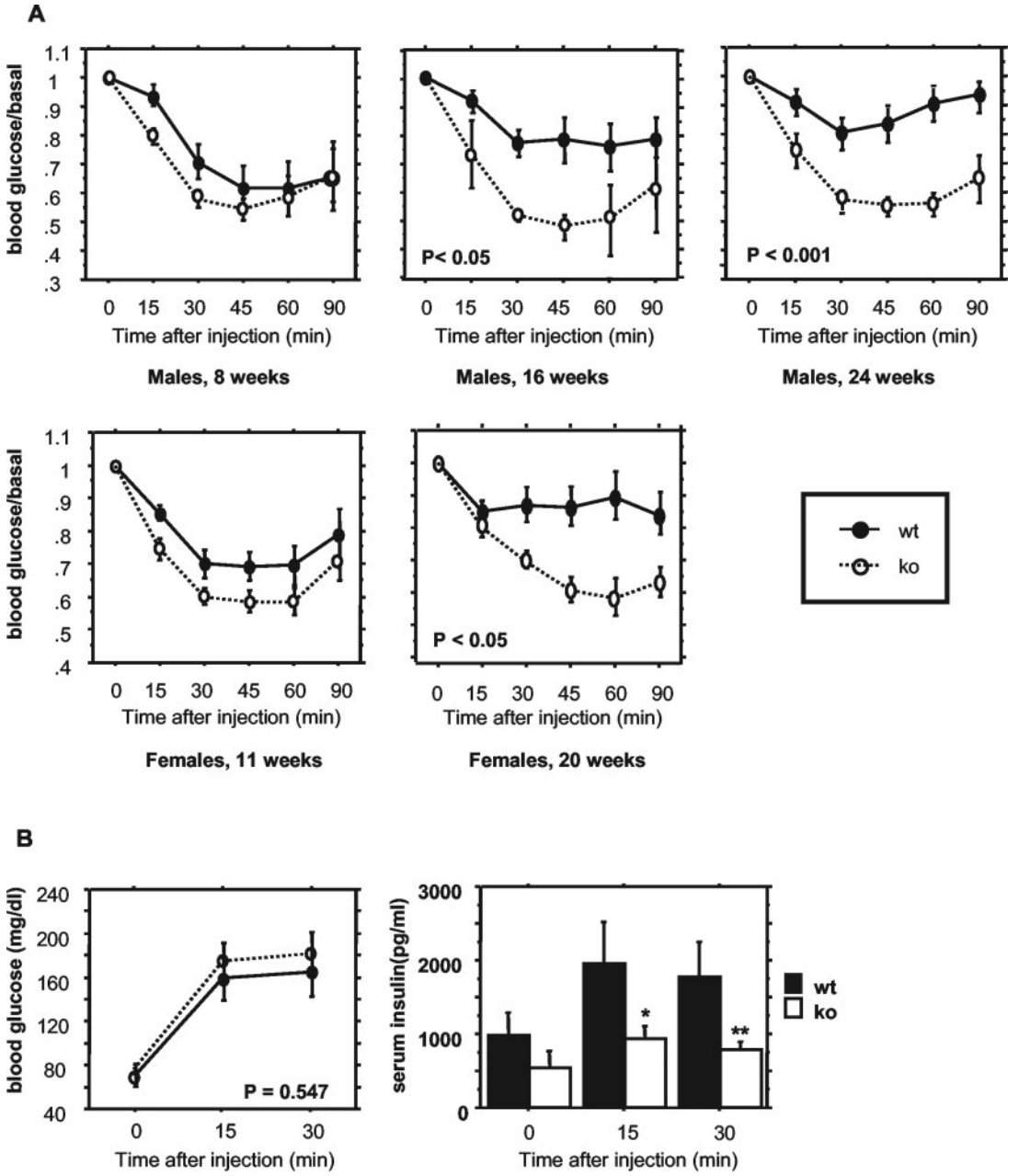

FIG. 3. PI5P4Kβ$^{-/-}$ mice are hypersensitive to insulin. (A) Insulin tolerance tests in male and female wild-type (wt) and knockout (ko) mice. Results are means ± standard errors of the mean of the blood glucose/basal blood glucose ratio from at least nine animals of each gender and genotype. *P* values were calculated by repeated-measures analysis of variance. (B) Glucose tolerance test and insulin measurements during the test in 7-month-old male mice (seven wild-type and eight knockout mice) (*, $P < 0.05$, and **, $P < 0.01$, compared to the wild type).

that older PI5P4Kβ$^{-/-}$ males had significantly less fat tissue than their wild-type littermates. Female PI5P4Kβ$^{-/-}$ mice had normal amounts of fat at all ages measured, even when they were fed a high-fat diet (Table 1).

Insulin hypersensitivity is not due to leanness. It has been well established that body fat affects insulin responsiveness (7). Thus, we investigated the possibility that the observed insulin hypersensitivity is caused by reduced fat accumulation. We examined fat content and insulin tolerance in young mice in which maturity-onset adiposity had not yet occurred. The PI5P4Kβ$^{-/-}$ mice in this group had statistically significant insulin hypersensitivity but no significant difference in body fat compared to wild-type littermates (Fig. 6). Thus, the increased insulin responsiveness observed in PI5P4Kβ$^{-/-}$ mice is not dependent on their reduced fat accumulation.

PI5P4Kβ$^{-/-}$ mice have normal leptin levels and normal food intake. We measured the food intake of wild-type and mutant mice and found no difference in the amount of food eaten by male mice of different genotypes between 4 and 6 weeks of age when normalized to body weight (data not shown).

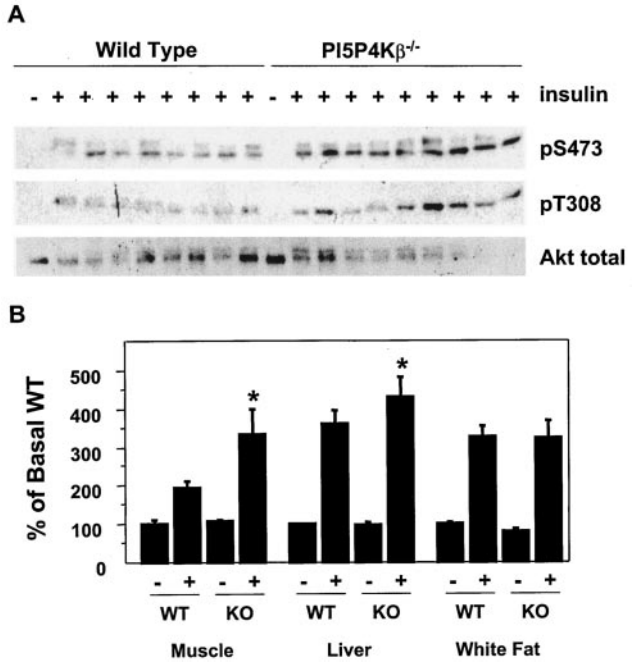

FIG. 4. Insulin-induced Akt activation is enhanced in skeletal muscle from PI5P4K$\beta^{-/-}$ mice. (A) Akt phosphorylation at serine 473 (pS473) and threonine 308 (pT308) and total Akt protein levels (note that the antibody reacts more strongly with nonphosphorylated Akt) in skeletal muscles from 5-month-old female wild-type and PI5P4K$\beta^{-/-}$ mice injected with saline or insulin. Each lane represents a single mouse. (B) Akt activity assays in tissues from wild-type and PI5P4K$\beta^{-/-}$ mice injected with saline or insulin (two to six unstimulated wild-type and knockout mice; five to nine wild-type and knockout mice injected with insulin; * $P < 0.05$). Results are means ± standard errors of the means and represent one of two experiments.

TABLE 1. Body fat content of PI5P4K$\beta^{+/+}$, PI5P4K$\beta^{+/-}$, and PI5P4K$\beta^{-/-}$ mice

Method	Gender	Genotype[a]	Age (wk)	Diet	% Body fat[b]	n
DEXAScan						
	Male	WT	10	Chow	17.2 ± 1.5	8
	Male	KO	10	Chow	16.0 ± 1.7	8
	Male	WT	26	Chow	31.1 ± 2.6	8
	Male	KO	26	Chow	21.6 ± 4.7**	8
	Female	WT	30	Chow	23.9 ± 6.9	6
	Female	KO	30	Chow	22.0 ± 5.8	6
Carcass analysis						
	Male	WT	36	Chow	38.7 ± 2.2	7
	Male	HET	36	Chow	30.5 ± 2.8*	6
	Male	KO	36	Chow	17.6 ± 2.5**,#	6
	Female	WT	21	Chow	18.3 ± 8.8	10
	Female	KO	21	Chow	17.7 ± 4.2	10
	Female	WT	36	High fat	47.6 ± 11.0	10
	Female	HET	36	High fat	38.9 ± 14.8	14
	Female	KO	36	High fat	41.0 ± 18.9	11

[a] WT, wild type; KO, knockout; HET, heterozygous.
[b] *, $P < 0.05$ compared to wild type; **, $P < 0.01$ compared to wild type; #, $P < 0.05$ compared to heterozygotes.

The hormone leptin has been shown to affect both feeding behavior and insulin responsiveness. Because leptin is secreted by fat cells, we measured leptin content in the serum of female mice, which do not have altered body fat composition. We measured the amount of leptin present in serum of wild-type and mutant mice either after an overnight fast or after ad libitum feeding overnight. Leptin levels in PI5P4K$\beta^{-/-}$ female mice were similar to those of wild-type littermates under both fed and fasting conditions. Furthermore, the leptin levels measured in both wild-type and mutant mice fit a similar linear relationship when compared with the mice's body weights, as expected (Fig. 7).

PI5P4K$\beta^{-/-}$ mice remain lean on a high-fat diet. PI5P4K$\beta^{-/-}$ mice that were fed a high-fat diet continuously from the time of weaning gained weight compared to PI5P4K$\beta^{-/-}$ mice on a regular chow diet but remained proportionally lighter than wild-type littermates on the high-fat diet (Fig. 8A). Additionally, PI5P4K$\beta^{-/-}$ mice remain more sensitive to insulin than wild-type littermates when fed a high-fat diet (Fig. 8B). Similar results were obtained for male and female mice. Chemical carcass analysis revealed that, as on the chow diet, male PI5P4K$\beta^{-/-}$ mice fed a high-fat diet had significantly less fat than wild-type littermates (mean body fat content for 11 wild-type male mice on the high-fat diet was 56.2% ± 6.2%; mean body fat content for 11 PI5P4K$\beta^{-/-}$ male mice on the high-fat diet was 37.4% ± 5.6%; $P = 0.04$), while the body fat content of female PI5P4K$\beta^{-/-}$ on a high-fat diet was similar to that of

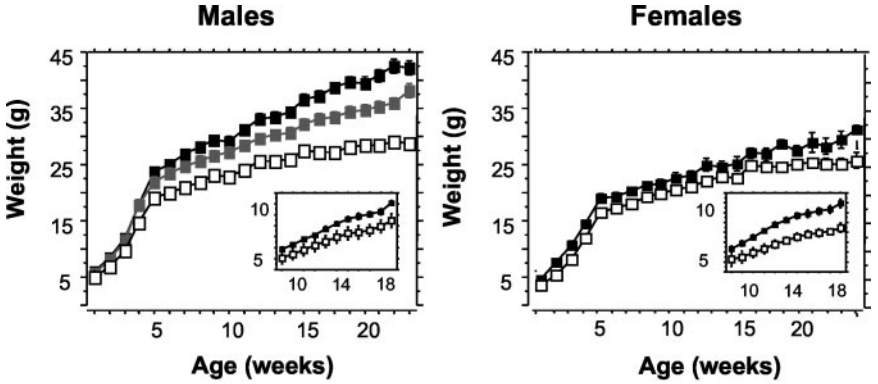

FIG. 5. PI5P4K$\beta^{-/-}$ mice exhibit growth retardation. Growth curves for wild-type (black squares), heterozygous (gray squares) and knockout (white squares) male and female mice (5 to 10 mice per genotype and gender). The data are mean body weights ± standard errors of the mean. The insets show the period from 9 to 19 days of age, with the *x* axis marked in days.

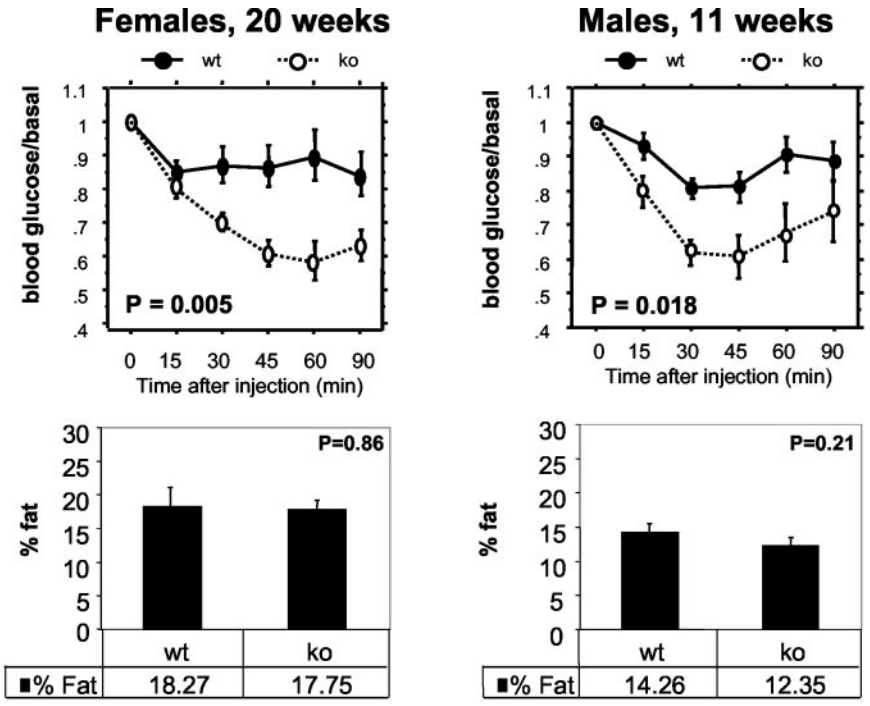

FIG. 6. Hypersensitivity to insulin is not caused by decreased adipose tissue content. Insulin tolerance tests and chemical carcass analysis were carried out for 20-week-old female mice and 11-week-old male mice. wt, wild-type mice; ko, PI5P4Kβ$^{-/-}$ mice. All results are means ± standard errors of the means for at least 9 animals of each genotype and gender.

wild-type littermates (see discussion of body fat composition above).

DISCUSSION

PI-5-P 4-kinases exist in all fully sequenced multicellular organisms, including the nematode *Caenorhabditis elegans* and the fruit fly *Drosophila melanogaster*, but are not present in unicellular organisms. This is the first demonstration of a physiological role for these enzymes in any organism. We have shown that mice lacking PI5P4Kβ are viable, mildly growth retarded, and hypersensitive to insulin; also, male PI5P4Kβ$^{-/-}$ mice have less fat than wild-type controls. Furthermore, we showed that the observed insulin hypersensitivity occurs before the reduced adiposity in male mice and independent of body fat content in female mice. Finally, we demonstrated that insulin-induced Akt activation is enhanced in skeletal muscle and liver but not in white adipose tissue from mice lacking PI5P4Kβ. Thus, PI5P4Kβ is important for determining whole-body insulin responsiveness in vivo regardless of body fat content.

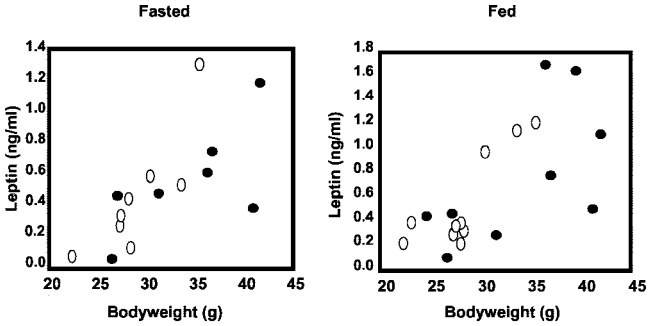

FIG. 7. PI5P4Kβ$^{-/-}$ mice produce normal amounts of leptin under fed and fasting conditions. Leptin was measured for 6-month-old female wild-type (filled circles) and PI5P4Kβ$^{-/-}$ mice (open circles), after fasting or feeding, and reported as a function of body weight. Results are reported for at least seven mice of each genotype and condition.

The molecular mechanism by which PI5P4Kβ reduces insulin responsiveness is not yet clear. PI-4,5-P_2, the product of PI5P4Kβ catalytic activity, is a substrate of PI3K for the production of PI-3,4,5-P_3. Thus, one might have expected that disruption of PI5P4Kβ would decrease insulin signaling, in contrast to what we found. However, it has been shown that overexpression of PI5P 4-kinases in cell culture decreases insulin-dependent Akt phosphorylations (8), which is consistent with our results in PI5P4Kβ$^{-/-}$ mice. Furthermore, exogenous expression of the bacterial phosphatase IpgD, which produces PI-5-P (25), stimulates the phosphorylation of Akt (8). These results raise the possibility that PI-5-P, the substrate of PI5P4Kβ, is required for maintaining PI-3,4,5-P_3 levels and Akt activation. Such a model would be consistent with the increased insulin sensitivity and increased Akt activation that we observe in PI5P4Kβ$^{-/-}$ mice.

PI5P4Kβ was originally cloned by association with the 55-kDa tumor necrosis factor receptor (TNFR1) (9). Tumor necrosis factor alpha, a ligand for TNFR1, has been shown to inhibit insulin signaling by an unknown mechanism, possibly involving serine phosphorylation of IRS1 (16, 27). TNFR1$^{-/-}$ mice are protected from obesity-induced insulin resistance

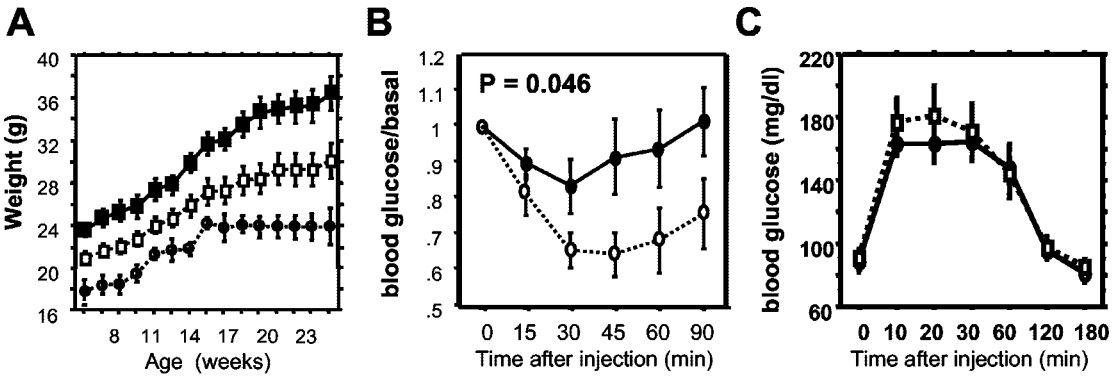

FIG. 8. PI5P4Kβ$^{-/-}$ mice remain hypersensitive to insulin on a high-fat diet. (A) Growth curves for wild-type female mice on a high-fat diet (filled squares; $n = 11$), PI5P4Kβ$^{-/-}$ female mice on a high-fat diet (open squares; $n = 15$), and PI5P4Kβ$^{-/-}$ female mice on a regular chow diet (open circles; $n = 6$). (B) Insulin tolerance test for wild-type (filled circles; $n = 6$) and PI5P4Kβ$^{-/-}$ (open circles, $n = 11$) 36-week-old female mice fed the high-fat diet continuously from the time of weaning. (C) Glucose tolerance test for wild-type (filled squares; $n = 6$) and PI5P4Kβ$^{-/-}$ (open squares; $n = 11$) 36-week-old female mice fed the high-fat diet continuously from the time of weaning. All results are means ± standard errors of the means.

(34). PI5P4Kβ may contribute to signaling downstream of TNFR1 that inhibits insulin response.

The inability of PI5P4Kα and PI5P4Kγ to compensate for the loss of PI5P4Kβ in the context of glucose homeostasis in mice may be explained by isoform-specific expression patterns, interaction partners, or subcellular localizations. It appears that a major factor in the insulin hypersensitivity resulting from loss of PI5P4Kβ is increased insulin signaling in muscle due to loss of PI5P4Kβ in muscle. The ratio of PI5P4Kβ expression to PI5P4Kα expression is particularly high in skeletal muscle, as seen in Fig. 2. Perhaps the closely related enzyme PI5P4Kα is able to compensate more effectively for the loss of PI5P4Kβ in tissues in which PI5P4Kα is more highly expressed, including white adipose tissue. However, the physiology of glucose homeostasis is controlled by complex communication between multiple tissues, including the brain (1, 4, 5, 18, 19, 24). It would be interesting to examine the isoform-specific and tissue-specific functions of PI-5-P 4-kinases in insulin signaling and glucose homeostasis further by generating mice lacking PI5P4Kβ in individual tissues, as well as by generating mice lacking other isoforms of PI-5-P 4-kinase.

Insulin stimulates the transport of glucose into both muscle and fat, where it is metabolized via glycolysis or converted to glycogen or triglycerides, the latter being the major form of adipose tissue accumulation. The increased insulin sensitivity of skeletal muscles in PI5P4Kβ$^{-/-}$ mice in the presence of normally insulin-responsive adipose tissue would likely lead indirectly to decreased transport of glucose into white adipose tissue because the increased insulin-stimulated glucose transport in muscle leads to a lower requirement for basal insulin secretion, as seen in Fig. 3B. This could explain the reduced adiposity in adult male mice lacking PI5P4Kβ. Consistent with this idea, decreased adiposity has also been observed in mice expressing transgenic activated Akt in muscle (David Glass, personal communication).

By measuring bone lengths, we found both male and female PI5P4Kβ$^{-/-}$ mice to be 5 to 10% shorter than wild-type mice at all ages, probably reflecting slower growth during embryogenesis or in the early postnatal period. The weight difference in male mice increases with age because the growth retardation effect is compounded by decreased fat accumulation in males. The overall growth retardation seems to occur early in life, and inhibition of PI5P4Kβ later in life may not affect growth. The non-Mendelian survival of PI5P4Kβ$^{-/-}$ newborn mice may be related to reduced embryonic growth rates in comparison to those of wild-type mice. Thus far, we have not observed decreased survival in PI5P4Kβ$^{-/-}$ adult mice. The insulin hypersensitivity, reduced adiposity, and lack of major anatomical or physiological defects observed thus far in adult PI5P4Kβ$^{-/-}$ mice make PI5P4Kβ an attractive target for the development of inhibitors that may be useful in the treatment of obesity and type 2 diabetes.

ACKNOWLEDGMENTS

We thank Harald Schulze of the Dana Farber Cancer Institute for antiserum raised against PI5P4Kα. We thank Tadaomi Takenawa for sharing an antibody against PI5P4Kγ. We thank John Watt, Nicole Logsdon, Nikki Madson, and Monica Kosmatka for assistance with breeding and genotyping PI5P4Kβ$^{-/-}$ mice. We thank Roderick Bronson and Derek Abbott for histological analysis of pancreatic islets. We thank Cyril Benes and Jonathan Hurov for critical reading of the manuscript.

This work was supported by NIH grants DK43051, DK60839, and DK57521 to B.B.K. and GM36624 to L.C.C. This investigation was supported by PHS research grant 5 P30 DK36836-15 from the National Institute of Diabetes and Digestive and Kidney Diseases.

REFERENCES

1. **Abel, E. D., O. Peroni, J. K. Kim, Y. B. Kim, O. Boss, E. Hadro, T. Minnemann, G. I. Shulman, and B. B. Kahn.** 2001. Adipose-selective targeting of the GLUT4 gene impairs insulin action in muscle and liver. Nature **409:**729–733.
2. **Accili, D., J. Drago, E. J. Lee, M. D. Johnson, M. H. Cool, P. Salvatore, L. D. Asico, P. A. Jose, S. I. Taylor, and H. Westphal.** 1996. Early neonatal death in mice homozygous for a null allele of the insulin receptor gene. Nat. Genet. **12:**106–109.
3. **Araki, E., M. A. Lipes, M. E. Patti, J. C. Bruning, B. Haag III, R. S. Johnson, and C. R. Kahn.** 1994. Alternative pathway of insulin signalling in mice with targeted disruption of the IRS-1 gene. Nature **372:**186–190.
4. **Bluher, M., M. D. Michael, O. D. Peroni, K. Ueki, N. Carter, B. B. Kahn, and C. R. Kahn.** 2002. Adipose tissue selective insulin receptor knockout protects against obesity and obesity-related glucose intolerance. Dev. Cell **3:**25–38.
5. **Bruning, J. C., D. Gautam, D. J. Burks, J. Gillette, M. Schubert, P. C. Orban, R. Klein, W. Krone, D. Muller-Wieland, and C. R. Kahn.** 2000. Role of brain insulin receptor in control of body weight and reproduction. Science **289:**2122–2125.
6. **Cantley, L. C.** 2001. Transcription. Translocating tubby. Science **292:**2019–2021.

7. **Carey, D. G., A. B. Jenkins, L. V. Campbell, J. Freund, and D. J. Chisholm.** 1996. Abdominal fat and insulin resistance in normal and overweight women: direct measurements reveal a strong relationship in subjects at both low and high risk of NIDDM. Diabetes **45:**633–638.
8. **Carricaburu, V., K. A. Lamia, E. Lo, L. Favereaux, B. Payrastre, L. C. Cantley, and L. E. Rameh.** 2003. The phosphatidylinositol (PI)-5-phosphate 4-kinase type II enzyme controls insulin signaling by regulating PI-3,4,5-trisphosphate degradation. Proc. Natl. Acad. Sci. USA **100:**9867–9872.
9. **Castellino, A. M., G. J. Parker, I. V. Boronenkov, R. A. Anderson, and M. V. Chao.** 1997. A novel interaction between the juxtamembrane region of the p55 tumor necrosis factor receptor and phosphatidylinositol-4-phosphate 5-kinase. J. Biol. Chem. **272:**5861–5870.
10. **Cho, H., J. Mu, J. K. Kim, J. L. Thorvaldsen, Q. Chu, E. B. Crenshaw III, K. H. Kaestner, M. S. Bartolomei, G. I. Shulman, and M. J. Birnbaum.** 2001. Insulin resistance and a diabetes mellitus-like syndrome in mice lacking the protein kinase Akt2 (PKB β). Science **292:**1728–1731.
11. **Clement, S., U. Krause, F. Desmedt, J. F. Tanti, J. Behrends, X. Pesesse, T. Sasaki, J. Penninger, M. Doherty, W. Malaisse, J. E. Dumont, Y. Le Marchand-Brustel, C. Erneux, L. Hue, and S. Schurmans.** 2001. The lipid phosphatase SHIP2 controls insulin sensitivity. Nature **409:**92–97.
12. **Divecha, N., O. Truong, J. J. Hsuan, K. A. Hinchliffe, and R. F. Irvine.** 1995. The cloning and sequence of the C isoform of PtdIns4P 5-kinase. Biochem. J. **309:**715–719.
13. **Elchebly, M., P. Payette, E. Michaliszyn, W. Cromlish, S. Collins, A. L. Loy, D. Normandin, A. Cheng, J. Himms-Hagen, C. C. Chan, C. Ramachandran, M. J. Gresser, M. L. Tremblay, and B. P. Kennedy.** 1999. Increased insulin sensitivity and obesity resistance in mice lacking the protein tyrosine phosphatase-1B gene. Science **283:**1544–1548.
14. **Fruman, D. A., F. Mauvais-Jarvis, D. A. Pollard, C. M. Yballe, D. Brazil, R. T. Bronson, C. R. Kahn, and L. C. Cantley.** 2000. Hypoglycaemia, liver necrosis and perinatal death in mice lacking all isoforms of phosphoinositide 3-kinase p85 alpha. Nat. Genet. **26:**379–382.
15. **Goldstein, B. J., A. Bittner-Kowalczyk, M. F. White, and M. Harbeck.** 2000. Tyrosine dephosphorylation and deactivation of insulin receptor substrate-1 by protein-tyrosine phosphatase 1B. Possible facilitation by the formation of a ternary complex with the Grb2 adaptor protein. J. Biol. Chem. **275:**4283–4289.
16. **Hotamisligil, G. S., P. Peraldi, A. Budavari, R. Ellis, M. F. White, and B. M. Spiegelman.** 1996. IRS-1-mediated inhibition of insulin receptor tyrosine kinase activity in TNF-α- and obesity-induced insulin resistance. Science **271:**665–668.
17. **Itoh, T., T. Ijuin, and T. Takenawa.** 1998. A novel phosphatidylinositol-5-phosphate 4-kinase (phosphatidylinositol-phosphate kinase IIγ) is phosphorylated in the endoplasmic reticulum in response to mitogenic signals. J. Biol. Chem. **273:**20292–20299.
18. **Kim, J. K., A. Zisman, J. J. Fillmore, O. D. Peroni, K. Kotani, P. Perret, H. Zong, J. Dong, C. R. Kahn, B. B. Kahn, and G. I. Shulman.** 2001. Glucose toxicity and the development of diabetes in mice with muscle-specific inactivation of GLUT4. J. Clin. Investig. **108:**153–160.
19. **Kitamura, T., C. R. Kahn, and D. Accili.** 2003. Insulin receptor knockout mice. Annu. Rev. Physiol. **65:**313–332.
20. **Klaman, L. D., O. Boss, O. D. Peroni, J. K. Kim, J. L. Martino, J. M. Zabolotny, N. Moghal, M. Lubkin, Y. B. Kim, A. H. Sharpe, A. Stricker-Krongrad, G. I. Shulman, B. G. Neel, and B. B. Kahn.** 2000. Increased energy expenditure, decreased adiposity, and tissue-specific insulin sensitivity in protein-tyrosine phosphatase 1B-deficient mice. Mol. Cell. Biol. **20:**5479–5489.
21. **Marcus, S. L., M. R. Wenk, O. Steele-Mortimer, and B. B. Finlay.** 2001. A synaptojanin-homologous region of Salmonella typhimurium SigD is essential for inositol phosphatase activity and Akt activation. FEBS Lett. **494:**201–207.
22. **Mauvais-Jarvis, F., R. N. Kulkarni, and C. R. Kahn.** 2002. Knockout models are useful tools to dissect the pathophysiology and genetics of insulin resistance. Clin. Endocrinol. (Oxford) **57:**1–9.
23. **Mauvais-Jarvis, F., K. Ueki, D. A. Fruman, M. F. Hirshman, K. Sakamoto, L. J. Goodyear, M. Iannacone, D. Accili, L. C. Cantley, and C. R. Kahn.** 2002. Reduced expression of the murine p85alpha subunit of phosphoinositide 3-kinase improves insulin signaling and ameliorates diabetes. J. Clin. Investig. **109:**141–149.
24. **Minokoshi, Y., C. R. Kahn, and B. B. Kahn.** 2003. Tissue-specific ablation of the GLUT4 glucose transporter or the insulin receptor challenges assumptions about insulin action and glucose homeostasis. J. Biol. Chem. **278:**33609–33612.
25. **Niebuhr, K., S. Giuriato, T. Pedron, D. J. Philpott, F. Gaits, J. Sable, M. P. Sheetz, C. Parsot, P. J. Sansonetti, and B. Payrastre.** 2002. Conversion of PtdIns(4,5)P(2) into PtdIns(5)P by the S. flexneri effector IpgD reorganizes host cell morphology. EMBO J. **21:**5069–5078.
26. **Rameh, L. E., K. F. Tolias, B. C. Duckworth, and L. C. Cantley.** 1997. A new pathway for synthesis of phosphatidylinositol-4,5-bisphosphate. Nature **390:**192–196.
27. **Rui, L., V. Aguirre, J. K. Kim, G. I. Shulman, A. Lee, A. Corbould, A. Dunaif, and M. F. White.** 2001. Insulin/IGF-1 and TNF-α stimulate phosphorylation of IRS-1 at inhibitory Ser307 via distinct pathways. J. Clin. Investig. **107:**181–189.
28. **Santagata, S., T. J. Boggon, C. L. Baird, C. A. Gomez, J. Zhao, W. S. Shan, D. G. Myszka, and L. Shapiro.** 2001. G-protein signaling through tubby proteins. Science **292:**2041–2050.
29. **Steele-Mortimer, O., L. A. Knodler, S. L. Marcus, M. P. Scheid, B. Goh, C. G. Pfeifer, V. Duronio, and B. B. Finlay.** 2000. Activation of Akt/protein kinase B in epithelial cells by the Salmonella typhimurium effector sigD. J. Biol. Chem. **275:**37718–37724.
30. **Tamemoto, H., T. Kadowaki, K. Tobe, T. Yagi, H. Sakura, T. Hayakawa, Y. Terauchi, K. Ueki, Y. Kaburagi, S. Satoh, et al.** 1994. Insulin resistance and growth retardation in mice lacking insulin receptor substrate-1. Nature **372:**182–186.
31. **Terauchi, Y., Y. Tsuji, S. Satoh, H. Minoura, K. Murakami, A. Okuno, K. Inukai, T. Asano, Y. Kaburagi, K. Ueki, H. Nakajima, T. Hanafusa, Y. Matsuzawa, H. Sekihara, Y. Yin, J. C. Barrett, H. Oda, T. Ishikawa, Y. Akanuma, I. Komuro, M. Suzuki, K. Yamamura, T. Kodama, H. Suzuki, T. Kadowaki, and et al.** 1999. Increased insulin sensitivity and hypoglycaemia in mice lacking the p85 alpha subunit of phosphoinositide 3-kinase. Nat. Genet **21:**230–235.
32. **Terebiznik, M. R., O. V. Vieira, S. L. Marcus, A. Slade, C. M. Yip, W. S. Trimble, T. Meyer, B. B. Finlay, and S. Grinstein.** 2002. Elimination of host cell PtdIns(4,5)P(2) by bacterial SigD promotes membrane fission during invasion by Salmonella. Nat. Cell Biol. **4:**766–773.
33. **Ueki, K., C. M. Yballe, S. M. Brachmann, D. Vicent, J. M. Watt, C. R. Kahn, and L. C. Cantley.** 2002. Increased insulin sensitivity in mice lacking p85β subunit of phosphoinositide 3-kinase. Proc Natl. Acad. Sci. USA **99:**419–424.
34. **Uysal, K. T., S. M. Wiesbrock, M. W. Marino, and G. S. Hotamisligil.** 1997. Protection from obesity-induced insulin resistance in mice lacking TNF-α function. Nature **389:**610–614.
35. **Whiteford, C. C., C. A. Brearley, and E. T. Ulug.** 1997. Phosphatidylinositol 3,5-bisphosphate defines a novel PI 3-kinase pathway in resting mouse fibroblasts. Biochem. J. **323:**597–601.
36. **Zambrowicz, B. P., G. A. Friedrich, E. C. Buxton, S. L. Lilleberg, C. Person, and A. T. Sands.** 1998. Disruption and sequence identification of 2,000 genes in mouse embryonic stem cells. Nature **392:**608–611.